Proceedings of the 4th International Conference on Applied Physics and Mathematical Modeling
DOI: 10.54254/2753-8818/2026.36566

Design and Performance Study of a Hexagonal Square-Ring Solar Absorber Based on Metasurface

Yichen Zhang

School of Optoelectronic Science and Engineering, University of Electronic Science and Technology of China, Chengdu, China
18180738138@163.com

Abstract. In order to utilize solar energy more effectively and alleviate energy difficulties, this paper proposes the use of a metasurface to construct a solar absorber. The materials used include a highly reflective TiN substrate, a SiO_2 dielectric layer, and a TiN hexagonal-prism ring pattern layer. Through simulation calculations using COMSOL software, it is shown that for the wavelength range of 300—1000 nm, the average absorption is 90.8%, and the absorption rate reaches 99.985% near 925 nm. Judging from the electric field distribution, the absorbed energy likely comes from surface plasmon polaritons or cavity resonance phenomena. After examining the absorption conditions under different parameters, it is found that within the studied range, the height of the pattern layer and the width of the hollow quadrangular prism have little effect on the absorption rate, and the absorption performance is stable. The designed structure itself is uncomplicated, capable of handling visible light and part of the infrared wavelengths, and has practical prospects for solar energy conversion.

Keywords: metasurface, solar energy, absorber, regular hexagonal square ring

1. Introduction

A metasurface is a type of two-dimensional artificial microstructure capable of precisely controlling light wavefronts at the sub-wavelength scale. It has evolved since the end of the 20th century from thoughts on negative refraction and other anomalous electromagnetic phenomena of metamaterials [1], and since the generalized Snell's law was proposed by Capasso's team at Harvard University in 2011 [2], it has become a highly promising direction in energy photonics. Its "phase discontinuity" mechanism provides a brand-new approach for improving the solar-to-thermal energy conversion efficiency [3]. In terms of practical applications, distributed seawater desalination and building heating are the most typical: the former utilizes the broadband absorption and thermal localization advantages of metasurfaces to convert solar energy into steam with an efficiency approaching 90%, thereby providing low-energy, decentralized water supply for remote areas [4]; the latter adopts a coordinated design of spectral directional absorption and infrared heat dissipation, making the efficiency of solar thermal coatings 15%—25% higher than before, which serves as a compact and lightweight solution for energy-saving retrofits in cold buildings [5].

DOI: 10.54254/2753-8818/2026.36566

However, currently, most known metasurface absorbers still suffer from the inherent defect of narrow-band response, failing to maintain near-blackbody absorption across the full solar spectrum [6], and high-temperature performance or batch manufacturing methods are not yet perfected. This greatly hinders the practical application of the envisioned scenarios [7], and therefore, finding broadband, durable, low-cost, and easily scalable metasurface technologies is a core task in advancing the development of new-generation photothermal energy [8].

Based on research in this field, this paper proposes a novel metasurface solar absorber design. The structure uses a pattern layer consisting of a regular hexagonal prism with a regular quadrangular prism removed from its center, under which a SiO_2 dielectric layer and a TiN substrate layer are sequentially placed [9, 10]. By setting appropriate periodic boundary conditions and corresponding wave excitation data in the COMSOL simulation environment, the absorption performance, stability, and other characteristics of the above absorber are explored. Simulation results show that under suitable conditions and geometric parameters, the absorption rate of this absorber can be maintained above 80% in the 300—1000 nm band, and can be maintained above 95% in longer wavelength bands.

2. Design and method

2.1. Structural design

The 3D model and unit structure of the metasurface absorber are shown in Figure 1. It consists of three layers: a TiN-based substrate at the bottom, which ensures that all incident light is absorbed within the patterned layer and has a thickness of H = 200 nm, a middle dielectric layer made of silicon dioxide, with a thickness of H_S = 100 nm, and an upper TiN patterned layer, which comprises a regular hexagonal prism with side length l = 200 nm, from which a regular square prism with side length L = 210 nm has been removed at its center and this patterned layer has a thickness of h = 150 nm. The patterned layer is arranged periodically on the surface of the silicon dioxide dielectric layer, with a periodicity of P = 550 nm, resulting in a highly symmetric structure. The surrounding medium of the metasurface is air, and the height of the air column is H_{air}= 1000 nm.

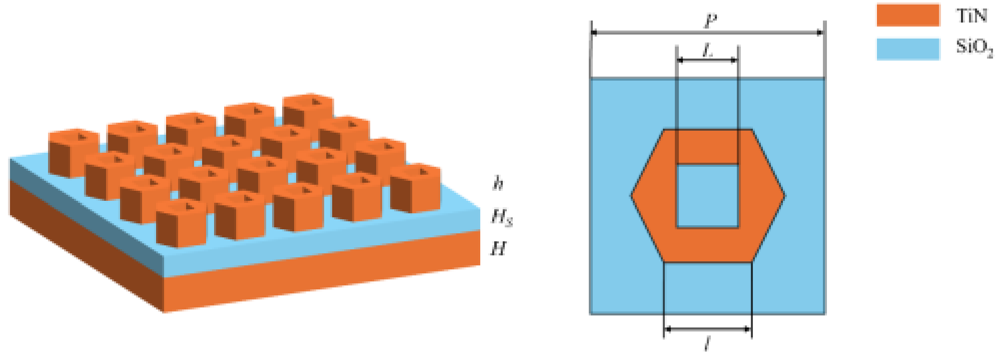

(a) 3D model schematic diagram (b) Top view of the structural unit

Figure 1. Schematic diagram of the absorber structure

DOI: 10.54254/2753-8818/2026.36566

2.2. Simulation settings

After completing the design, COMSOL software is used to explore the absorption performance of the absorber and the impact of certain geometric parameters on its absorption performance. In the software, periodic conditions are selected for two pairs of opposite outer surfaces perpendicular to the *xOy* plane; furthermore, Perfectly Matched Layers (PML) with a height of 400 nm are set above and below each unit structure in the *z*-axis direction to eliminate boundary scattering. Simultaneously, the inner surfaces of the two PMLs are set as wave excitation ports, with the power flow direction set downwards, the upper port open, and the lower port closed. Thus, the absorption rate of the absorber is calculated:

$$A = 1 - T - R \tag{1}$$

where T is the transmittance and R is the reflectance. Given the opaque TiN substrate, T is approximately 0, allowing A to be expressed as:

$$A = 1 - R \tag{2}$$

3. Results and discussion

3.1. Absorption performance

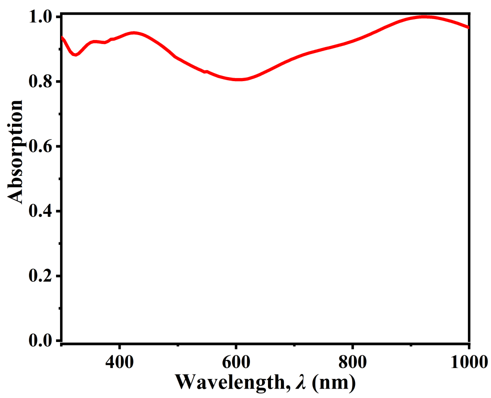

Figure 2. The absorption curve of the absorber

After adjusting some geometric parameters and performing data calculations, at *h*=150 nm and *L*=210 nm, the absorption rate is greater than 80% across the entire 300—1000 nm band, and the maximum average absorption rate is 90.8%. The results are shown in Figure 2. Among them, the absorption rate is greater than 90% for more than half of the wavelengths, and reaches a maximum of 99.985% at 925 nm; another obvious extreme absorption rate also reaches 95%. And the absorption rates for wavelengths greater than 830 nm all exceed 95%, indicating a high and relatively stable overall absorption rate. Although there is a noticeable drop in the absorption rate near the 600 nm band, the absorption amplitude is within an acceptable range, and the overall absorption rate remains high.

DOI: 10.54254/2753-8818/2026.36566

3.2. Analysis of the absorption mechanism through electric field distribution

To clarify the mechanism underlying the absorption, the electric field intensity of the pattern layer cross-section corresponding to the maximum absorption rate (925 nm) is analyzed, as shown in Figure 3. From the figure, it can be seen that the square ring itself is an area with a weaker electric field, an inhibition zone, or a shielding zone, while its outer edges, inner edges, and various sharp corners all show significant electric field enhancement. This special field distribution precisely explains the resonance absorption phenomenon of the absorber for near-infrared wavelengths [11]. The strong light spots seen at the edges and four corners suggest that the structure has mobilized localized surface plasmons or cavity resonance, at which time the light energy is highly concentrated and propagates within a small range [12, 13]. The highly reflective material used for the square ring forces the light to return along the normal direction, thereby lengthening the optical path and reducing transmission [14]. The discussion regarding the combination of the strong edge field and the central standing wave node provides a complete answer to the impedance matching issue [15], and clearly points out that the high efficiency of absorption in the 925 nm band serves as the fundamental physical guarantee for solar energy utilization.

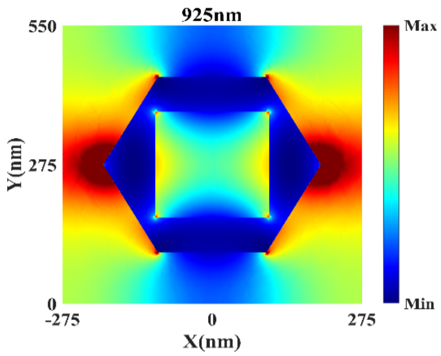

Figure 3. The electric field diagram of the cross-section in 925nm wavelength

3.3. Analysis of the influence of different geometric parameters

The impact of the geometric parameters on the absorber is vital. In this paper, the controlled variable method is used to explore the influence of geometric parameters on the absorption performance of the absorber.

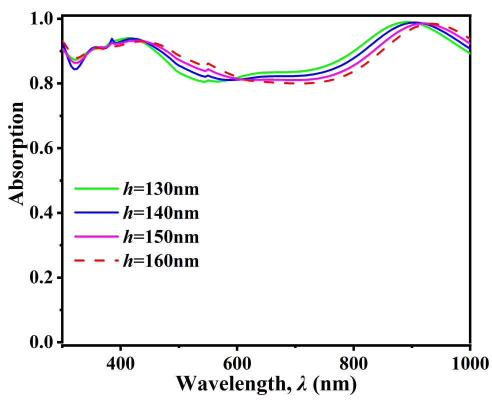

Figure 4. Absorption rate curves of different pattern layer thicknesses

DOI: 10.54254/2753-8818/2026.36566

Figure 4 shows the influence of the height of pattern layer *h* on the performance. When the height of the pattern layer varies between 130 nm and 160 nm, the absorption curve doesn't fluctuate significantly. It can be seen that the absorption peak shifts slightly but the overall variation trend of the absorption rate remains unchanged. And the average absorption rates are all relatively high, maintained above 89%, with the lowest absorption rate also remaining above 80%. In conclusion, minor errors in the height of the pattern layer have little impact on the performance of the absorber.

As shown in Figure 5, with the edge length of regular square prism *L* increasing, the positions of the absorption peak hardly change and the overall shape of the absorption curve remains stable. There is only a small change in the absorption value at each wavelength. Also, the absorption level in the full band still remains high, average above 90%, and the minimum value stays above 80% throughout the sweep. The performance is vital to the practical application because electron-beam lithography typically introduces corner rounding and edge roughness in high-aspect-ratio square apertures, both of which are tolerated by the present design. In contrast to solid nanopillars, the annular topology redistributes current density away from the central region, thereby reducing sensitivity to dimensional drift at the inner boundary.

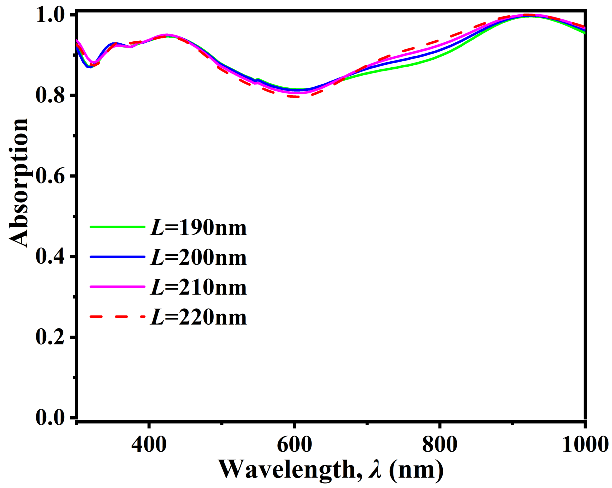

Figure 5. Absorption rate curves for different edge lengths of regular square prisms

Considering the impact of the above two parameters on the absorption performance, it can be concluded that slight changes in these two parameters may cause the absorption rate at the peaks and some wavelengths to change, but the overall performance does not show particularly obvious attenuation, verifying that there is a certain manufacturing tolerance adaptation space for these parameters.

4. Conclusions and outlook

The study innovatively designed a metasurface solar absorber based on a regular hexagon with a hollowed-out square, comprising a square ring pattern layer, a silicon dioxide dielectric layer, and a titanium nitride substrate reflection layer from top to bottom. Through theoretical simulation demonstration, the structure achieved an average absorption rate of 90.8% in the 300—1000 nm band, showing its comparable efficiency. Its high absorption performance stems from the synergistic coupling effect of surface plasmon resonance and guided mode resonance, a mechanism that was confirmed by the electric field diagram. The geometric parameter tolerance analysis shows that

DOI: 10.54254/2753-8818/2026.36566

when the pattern layer thickness and the edge lengths of regular square prisms vary within an appropriate range, only absorption peaks and values alter.

Compared with traditional structures, this design has a regular geometric shape, is easy for micro-nano processing, possesses stable performance, and has a high tolerance for minor parameter errors.

Future research can focus on multiple aspects. Improve the materials without excessively increasing costs, while maintaining or even enhancing the absorption performance, especially near 600nm wavelength. Additionally, the dimensions of the regular hexagonal prism and the regular quadrangular prism, as well as the thickness of each layer, are expected to be optimized to widen the absorption bandwidth, covering the full solar spectrum. The study is a feasible attempt for solar energy utilization and holds application prospects in solar energy conversion technologies.

References

[1] Engheta, N., & Ziolkowski, R. W. (2006). *Metamaterials: Physics and engineering explorations*. Wiley-IEEE Press. https://www.wiley.com/en-ir/Metamaterials%3A+ Physics+ and+Engineering+Explorations-p-00029415

[2] Yu, N., Genevet, P., Kats, M. A., Aieta, F., Tetienne, J.-P., Capasso, F., & Gaburro, Z. (2011). Light propagation with phase discontinuities: Generalized laws of reflection and refraction. *Science, 334*(6054), 333–337. https://doi.org/10.1126/science.1210713

[3] Yu, N., & Capasso, F. (2014). Flat optics with designer metasurfaces. *Nature Materials, 13*(2), 139–150. https://doi.org/10.1038/nmat3839

[4] Zhong, H., Liu, Z., Tang, P., Liu, X., Zhan, X., Pan, P., & Tang, C. (2020). Thermal-stability resonators for visible light full-spectrum perfect absorbers. *Solar Energy, 208*, 445–450. https://doi.org/10.1016/j.solener.2020.08.032

[5] Kim, I., So, S., Rana, A. S., Mehmood, M. Q., & Rho, J. (2018). Thermally robust ring-shaped chromium perfect absorber of visible light. *Nanophotonics, 7*(11), 1827–1833. https://doi.org/10.1515/nanoph-2018-0095

[6] Habil, M. K., Ghahremani, M., & Zapata-Rodríguez, C. J. (2022). Multi-octave metasurface-based refractory superabsorber enhanced by a tapered unit-cell structure. *Scientific Reports, 12*(1), 17066. https://doi.org/10.1038/s41598-022-21234-8

[7] Lee, D., Go, M., Kim, M., Jang, J., Choi, C., Kim, J. K., & Rho, J. (2021). Multiple-patterning colloidal lithography-implemented scalable manufacturing of heat-tolerant titanium nitride broadband absorbers in the visible to near-infrared. *Microsystems & Nanoengineering, 7*(14), 1–8. https://doi.org/10.1038/s41378-020-00237-8

[8] Mehrabi, S., Muhammad, R., Bilal, H., Naveed, M. A., & Ali, M. M. (2022). Ultra-broadband nanostructured metamaterial absorber based on stacked square-layers of TiN/TiO_2. *Optical Materials Express, 12*(6), 2199–2211. https://doi.org/10.1364/OME.455566

[9] Sun, C., Liu, H., Yang, B., Zhang, K., Zhang, B., & Wu, X. (2023). An ultra-broadband and wide-angle absorber based on a TiN metamaterial for solar harvesting. *Physical Chemistry Chemical Physics, 25*(1), 806–812. https://doi.org/10.1039/d2cp04976g

[10] Go, M., Lee, D., Kim, S., Jang, J., Kim, K.-W., Lee, J., Shim, S., Kim, J. K., & Rho, J. (2023). Facile fabrication of titanium nitride nanoring broadband absorbers in the visible to near-infrared by shadow sphere lithography. *ACS Applied Materials & Interfaces, 15*(2), 3266–3273. https://doi.org/10.1021/acsami.2c17875

[11] Huo, D., Zhang, J., Wang, Y., Wang, C., Su, H., & Zhao, H. (2018). Broadband perfect absorber based on TiN-nanocone metasurface. *Nanomaterials, 8*(7), 485. https://doi.org/10.3390/nano8070485

[12] Huo, D., Zhang, J., Wang, H., Ren, X., Wang, C., Su, H., & Zhao, H. (2017). Broadband perfect absorber with monolayer MoS_2 and hexagonal titanium nitride nano-disk array. *Nanoscale Research Letters, 12*, 465. https://doi.org/10.1186/s11671-017-2170-9

[13] Huo, D., Ma, X., Su, H., Wang, C., & Zhao, H. (2021). Broadband absorption based on thin refractory titanium nitride patterned film metasurface. *Nanomaterials, 11*(5), 1092. https://doi.org/10.3390/nano11051092

[14] Piao, R.-Q., Xu, Q., Wong, W.-H., Pun, E. Y.-B., & Zhang, D.-L. (2019). A theoretical study of broadband nearly perfect metasurface absorber based on nanoarray of titanium nitride. *Advanced Theory and Simulations, 2*(7), 1900042. https://doi.org/10.1002/adts.201900042

[15] Liu, H., Yang, B., Zhang, K., Zhang, B., & Wu, X. (2023). Impedance matching and optical path enhancement in refractory TiN metamaterial absorbers. *Journal of Physics D: Applied Physics, 56*(18), 185105. https://doi.org/10.1088/1361-6463/acb8d2